

# The Viscoelastic Coarse-Grained Dynamic Model of the Polymer Network with Embedded Rod-Like Particles. Relaxation Spectra and Mobility of Different Scales.

Yuli Ya. Gotlib,\* Isaak A. Torchinskii, Vladimir P. Toshchevikov, Vladimir A. Shevelev

**Summary:** The viscoelastic coarse-grained dynamic model of a polymer network with rod-like particles included into the network is considered. The rods are regularly distributed in the network. The entanglements of rods in a polymer network lead to quasielastic interactions between the rods and network fragments. The structure of the relaxation spectrum is considered. The dependence of the relaxation properties of the network with included rods on the viscoelastic parameters of the network without rods, on the length and the friction of the rods are investigated at different strength of the interaction between rods and network fragments. The differences between collective types of relaxation of the rods and the network and localized motions of the rods on the background of immobile network fragments are discussed. The results of the theory are applied to the description of the rotational and translational motions of the rods appearing in dielectric relaxation, NMR and other phenomena.

**Keywords:** dielectric relaxation; NMR; polymer networks; relaxation spectra; rod-like inclusions

## Introduction

Polymer networks and gels containing hard rod-like particles were synthesized and experimentally investigated by Khokhlov, Wegner, Philippova, Fytas and their coauthors.<sup>[1–5]</sup> The polyelectrolyte gels of such structure possess high swelling capacity in water and can be applied to medicine, agriculture and food industry as functional materials (e.g. sensors, carriers of drugs, membranes with regulated permeability etc.). The dielectric, NMR and mechanical relaxation of such systems were modeled by simple viscoelastic models and investigated by the authors.<sup>[6–13]</sup>

In this paper we present the more detailed description of the relaxation spectrum of the viscoelastic model used previously, discuss the structure of the different branches of this spectrum depending on the parameters of the model including the possible chain stretching between junctions (or swelling of the network). We discuss in more detailed way the behavior of the normal modes with moving or fixed junctions of the network.

The model physical treatment of the elastic Gaussian polymer network with included hard rod-like particles is based on the replacing of the rod by the viscoelastic element. The mean-square length of the element is equal to the length of the rod. The viscous properties of the rod (or hard dumbbell) are described by introducing the internal friction in the quasielastic dumbbell. In this approximation, the following

Institute of Macromolecular Compounds, Russian Academy of Sciences, Bolshoi Prospekt 31, V.O., St.-Petersburg, 199004, Russia  
E-mail: yygoteib@imc.macro.ru

condition should be fulfilled. The ratio of the coefficients of translational and rotational diffusion of the model elastic dumbbell must be equal to this ratio for hard dumbbell. This approach was proposed and used by Darinskii, Gotlib, Klushin, Neelov, Lyulin<sup>[14–17]</sup> and was confirmed by some computer simulations.<sup>[16,17]</sup> From mathematical point of view this approach corresponds to the replacing of the Lagrange multipliers in the equation of motion for hard rods by their average values.<sup>[14]</sup> We emphasize here on the method of calculation of this average Lagrange multiplier (or effective elastic constant) for a rod included into a polymer network as a function of elastic network parameters, the coupling between network and rod and of the length of rod. Then we consider the behaviour of the relaxation spectrum of the complex system “network-rods” also taking into account the chain stretching between junctions in a swollen polymer network.

### Model of a Polymer Network with Included Rods

As it was shown in the experiments by Khokhlov, Philippova, Zaroslov et al.,<sup>[1–5]</sup> the length of rods,  $l$ , which are steady included in the network is greater than the distance between neighboring junctions  $h_0$ , i.e. greater than the dimension of the cell of

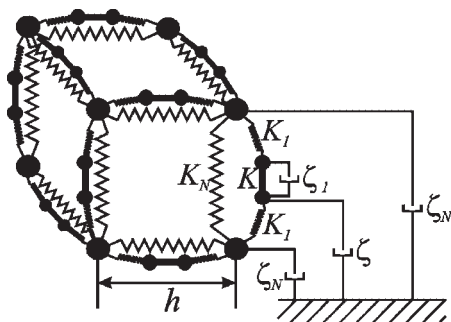


**Figure 2.**

The cell of 3-dimensional regular cubic network model with included rods.

the network (see Figure 1). Since the motions of such comparatively long rods are affected mainly by the network motions, the scale of which is equal or greater than the length of the rod,<sup>[1–5]</sup> it was proposed to introduce the “renormalized” network.<sup>[11–13]</sup> In this approach, the real network is divided on the regions of the scale equal to the distance between neighboring rods (Figure 2). For this approximation it was shown<sup>[11]</sup> that if the cell of the renormalized coarse-grained network consists of  $n$  cells of primary network, the effective elasticity constant,  $K_N$ , of the renormalized network will be  $n$ -times greater than the constant,  $K_{N0}$ , of the primary network and the effective friction constant of the

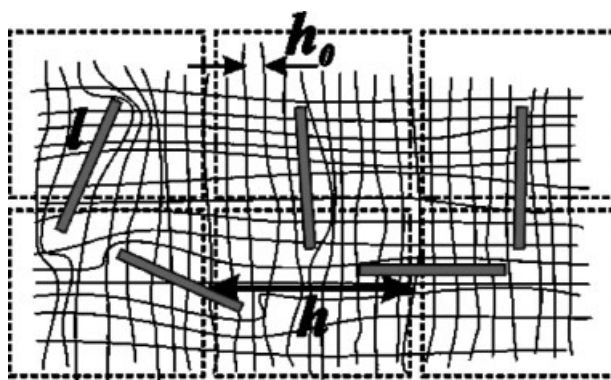


**Figure 1.**

A polymer network with long included rod-like particles.  $n = h/h_0$ .

junction of the renormalized network,  $\zeta_N$ , will be by the factor  $n^3$  greater than the friction,  $\zeta_{N0}$ , of the junction in a primary network. We remind that the friction of the junction in the primary cubic network,  $\zeta_{N0}$ , is equal to the total friction of the 3 chains (or 6 “half-chains”) attached to one junction and  $K_{N0}$  is equal to the elastic constant of the chain connecting two neighboring junctions. We remind also that in these network models we consider the space scales and processes (elasticity and times) in the scale of chains (and not chain segments), i.e. we consider relatively long-scale processes. The possibility to consider separately the intrachain and interchain long-scale processes in polymer networks and to use corresponding network models was found previously.<sup>[18,19]</sup>

In our model for relatively long rods the coefficients  $\zeta_N$  and  $K_N$  present average friction and relative elasticity of the domains of primary network. The bead-and-spring model of the coarse-grained renormalized network with included rods is presented on Figure 2. The effects of topological entanglements of rods in a polymer network (when rods move together with network fragments) are taken into account by elastic potential that prevents the translational displacements of the rods on the distances greater than the average distance between rods and hinders the rotational mobility of the rods. In the coarse-grained model (Figure 2) this potential acts between the rod ends and the centers of network domains and is characterized by the elasticity constant,  $K_1$ . The quasi-elastic potential of such type may be caused by the entropic and other forces (due to entanglements) in network strands when they are stretched and carried away by the moving rods. The effective spring constant,  $K$ , presents the average value of the Lagrange multiplier for the rod.

The next problem is to evaluate the constant  $K$ , because now the mean-square dimension of the spring imitating the rod depends on the surrounding springs (the elements of the network,  $K_1$  and  $K$  for other rods). The value of  $K$  is determined from

the equality of the mean-square length of the spring modeling the rod to the length of the rod. If we also take into account the average linear stretching of chains between junctions and corresponding average stretching of the rods between junctions,  $\langle \Delta l \rangle$ , we obtain the following equation

$$l^2 = \langle \Delta l^2 \rangle + \langle \Delta l \rangle^2. \quad (1)$$

The value of  $\langle \Delta l \rangle$  has a simple form<sup>[10–13]</sup>

$$\langle \Delta l \rangle = h \frac{K_1}{K_1 + 2K}, \quad (2)$$

where  $h$  is the average distance between neighboring junctions in the model, Figure 2.

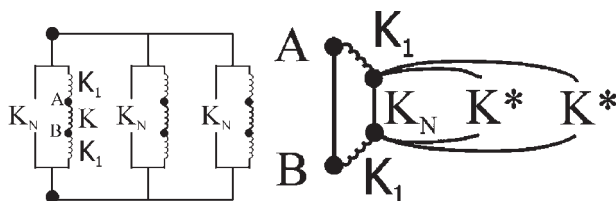
The quantity  $\langle \Delta l^2 \rangle$  in Equation (1) is the mean-square fluctuation of the length of the spring modeling the rod. The direct way to calculate the  $\langle \Delta l^2 \rangle$  as a function of  $K$ ,  $K_1$ ,  $K_N$  was realized in<sup>[11–13]</sup> using the normal modes of the model presented on Figure 2. In the present paper we propose a more simple method for calculation of  $\langle \Delta l^2 \rangle$  by means of mechanical treatment of the combination of springs forming our dynamic visco-elastic model. In some papers<sup>[18–20]</sup> it was shown that the mean-square distance between neighboring junctions in a cubic network built from springs with elasticity constant  $K^*$  is

$$\langle \Delta h^2 \rangle = kT/K^*, \quad (3)$$

i.e. is three times smaller than the value  $\langle \Delta h^2 \rangle_{\text{free spring}} = 3kT/K^*$  for the same free spring not included into the network. This means that the surrounding network acts on the spring between neighboring junctions as two additional springs, so that the elastic constant is 3 times greater. In our case the effective elastic constant  $K^*$  between junctions is

$$K^* = K_N + \frac{KK_1}{K_1 + 2K}. \quad (4)$$

The picture of the effective spring in our network model is presented in Figure 3. Taking into account the position of springs (in line or parallel) we easily obtain the effective elasticity of the complex spring

**Figure 3.**

Effective elasticity elements.

connecting points A and B as

$$K_{AB} = K + \left[ \frac{2}{K_1} + \frac{1}{K_N + 2K^*} \right]^{-1}$$

$$= K + \left[ \frac{2}{K_1} + \frac{1}{3K_N + 2KK_1/(K_1 + 2K)} \right]^{-1}. \quad (5)$$

The mean-square fluctuation of the length of the elastic element modeling the rods is

$$\langle \Delta l^2 \rangle = 3kT/K_{AB}. \quad (6)$$

Using Equations (2), (5) and (6), the condition (1) for the elasticity constant  $K$  is rewritten as follows

$$l^2 = h^2 \left( \frac{K_1}{K_1 + 2K} \right)^2 + \frac{3kT}{K + \left[ \frac{2}{K_1} + \frac{1}{3K_N + 2KK_1/(K_1 + 2K)} \right]^{-1}}. \quad (7)$$

This result coincides with the rigorous calculation from normal coordinate treatment.<sup>[11–13]</sup> Using Equation (7) one can calculate the elasticity constant  $K$  as a function of the parameters  $K_1$ ,  $K_N$  and  $h/l$ . The dependences  $K = K(K_1)$  at different values of  $K_N$  and  $h/l$  are plotted in Figure 4.

Using the estimated values of  $K$  one can investigate the relaxation spectrum of the network with included rods as a function of the parameters of our network model ( $K_1$ ,  $K_N$ ,  $\zeta_N$ ,  $h$ ). In our description we use the relationship  $\zeta_1 = \zeta/4$  that corresponds to the equality of the coefficients of translational and rotational diffusion of the elastic dumbbell to the corresponding

coefficients of the hard dumbbell.<sup>[14–17]</sup>

Moreover, we note that the possible values of  $K_1$  (the strength of the interaction between the rods and network fragments due to entanglements of rods in a polymer network) can be estimated using some general physical argumentations. The rod may be strongly enough included in the cell of the “renormalized” coarse-grained network if the length of the rod,  $l$ , is much greater than the size of the cell of the primary network,  $l > h_0$ . If  $l < h_0$ , the rod will interact mainly with one chain (or be sorbed on the chain), or it can diffuse through the network. In our model we consider the case when the rod cannot go out from the cell of the renormalized network,  $h$ . This means that the mean square displacement of a rod may be smaller (or not greater) than  $h$ , that imposes some restrictions on the value of  $K_1$ . The mean-square displacement of the centre of the rod,  $\langle \Delta r^2 \rangle$ , as a function of  $K_1$  was estimated in ref.<sup>[11]</sup> for the considered model:

$$\langle \Delta r^2 \rangle = \frac{3kT}{2K_1} + \frac{kT}{K_N + KK_1/(K_1 + 2K)}. \quad (8)$$

Thus, for satisfying the inequality  $\langle \Delta r^2 \rangle < h^2$ , the condition  $3kT/2K_1 < h^2$  is required. Furthermore, we propose that  $l$  is some smaller or equal to  $h$  ( $l \leq h$ ) because in opposite case the rods should be overlapped and we have to consider direct interaction between rods. Therefore, in our considerations we will use the condition,  $K_1 > 3kT/2l^2$ , which at  $l \leq h$

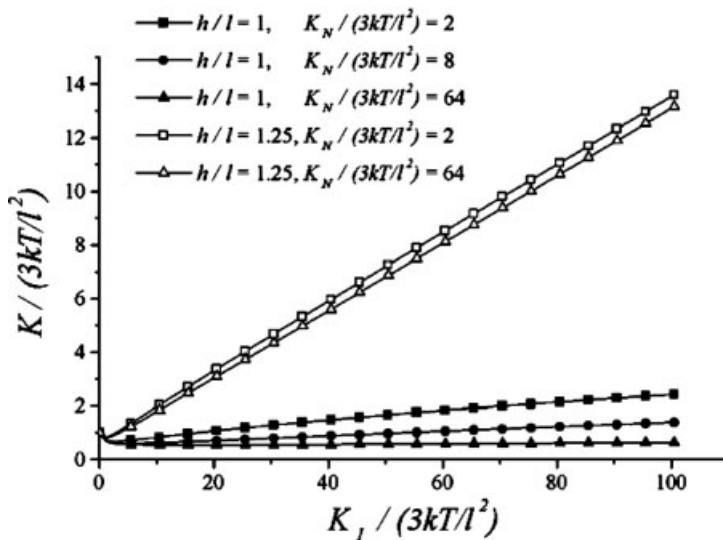


**Figure 4.**

The values of the elasticity constant  $K$  as functions of the parameters  $K_1/(3kT/l^2)$ ,  $K_N/(3kT/l^2)$  and  $h/l$ .

leads to the inequality,  $3kT/2K_1 < h^2$ , which is required for the condition  $\langle \Delta r^2 \rangle < h^2$ .

The equations of motion for the proposed network model are presented by a set of linear first-order differential equations for 7 variables belonging to one cell (see Equation (4) in ref.<sup>[11]</sup>). These equations can be reduced to three interconnecting equations for collective branches and to two double-degenerated equations for branches of motion of the rods at fixed network junctions. As it was shown in ref.<sup>[11]</sup> the total characteristic equation for the eigenvalues  $\lambda$  (or inverse relaxation times) at given phase shift  $\vec{\theta}(\theta_1, \theta_2, \theta_3)$  between the motions of the neighboring cells can be presented in the form<sup>[11]</sup>

$$(\tau_l^{-1} - \lambda)^2 (\tau_r^{-1} - \lambda)^2 \left( (a - \lambda)(\tau_l^{-1} - \lambda)(\tau_r^{-1} - \lambda) - \frac{(\tau_l^{-1} - \lambda)3K_1^2(1 - X)}{(\zeta + 2\zeta_1)\zeta_N} - (\tau_r^{-1} - \lambda) \frac{3K_1(1 + X)}{\tau_l\zeta_N} \right) = 0 \quad (9)$$

Here  $\tau_r$  and  $\tau_l$  are the two relaxation times for damped rotation-vibration motion of the rod,

$$\tau_r = \frac{\zeta + 2\zeta_1}{K_1 + 2K}, \quad (10)$$

and for damped translation-vibration motion of the rod,

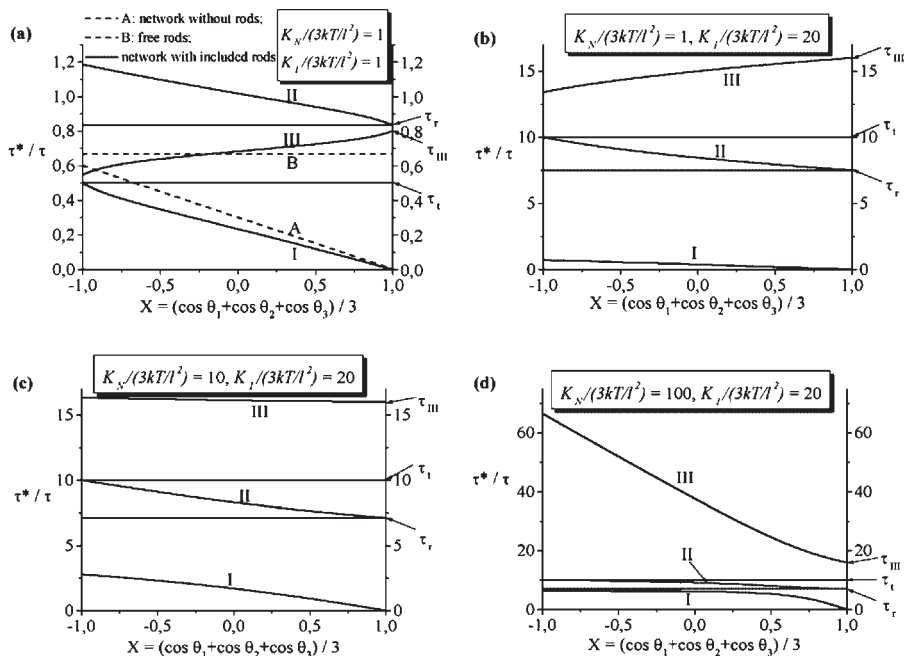
$$\tau_l = \frac{\zeta}{K_1}, \quad (11)$$

The parameters  $a$  and  $X$  in Equation (9) have the following form

$$a = \frac{6K_1 + 6K_N(1 - X)}{\zeta_N}, \quad X = X(\vec{\theta}) = \frac{\cos \theta_1 + \cos \theta_2 + \cos \theta_3}{3}. \quad (12)$$

Using Equation (9), we have calculated the relaxation spectrum of a polymer network with included rods at different viscoelastic parameters of the model. The results are presented in Figures 5a–d. As it can be seen from Figure 5a, the interaction

between the rods and network fragments leads to the fine structure of the relaxation spectrum as compared with the system of non-interacting network and rods. The system of non-interacting network and rods is characterized by one network branch of

**Figure 5.**

The relaxation spectra  $\tau(\vec{\theta})$  at different values of  $K_i/(3kT/l^2)$  and  $K_N/(3kT/l^2)$ .  $h/l = 1$ ,  $\zeta_N/\zeta = 10$ . The solid lines I, II, III correspond to the collective branches of the relaxation spectrum for a polymer network with included rods and  $\tau_r = (\zeta + 2\zeta_i)/(K_1 + 2K)$ ,  $\tau_t = \zeta/K_i$ ,  $\tau_{III} = \tau_t/(1 + 6\zeta/\zeta_N)$ ,  $\tau^* = l^2\zeta/6kT$ . Dashed lines illustrate the relaxation spectrum for the system of non-interacting network and rods.

the relaxation spectrum (dashed line A in Figure 5a) and by the rotational relaxation time of the rod,  $\tau_0 = l^2\zeta/4kT$  (dashed line B in Figure 5a). As it can be seen from Figures 5a–d (see also Equation (9)), the set of the relaxation times for the network with included rods,  $\tau(\vec{\theta}) = 1/\lambda(\vec{\theta})$ , contains the two twice-degenerated relaxation times  $\tau_r$  and  $\tau_t$ . Moreover, the relaxation spectrum includes 3 collective branches of the relaxation times which correspond to solutions of the cubic equation corresponding to the third multiplier in the left-hand side of Equation (9). The relaxation times of 3 collective branches depend on the wave vector  $\vec{\theta}(\theta_1, \theta_2, \theta_3)$ .

At in-phase motions of elements in adjacent cells (at  $\vec{\theta} \rightarrow 0$  or  $X \rightarrow 1$ ), each of the three collective branches (I, II, III) of the relaxation spectrum is characterized by a certain type of the movement of rods and

network fragments. The branch I is characterized at  $\vec{\theta} \rightarrow 0$  by infinitely long times,  $\tau(\vec{\theta}) \rightarrow \infty$ , and corresponds to in-phase *translational* mobility of the network fragments in adjacent cells when movements of network junctions and rod centers in the same cell are also in-phase. The characteristic motions of the branch II at  $\vec{\theta} \rightarrow 0$  correspond to in-phase *rotational* movement of rods in adjacent cells in the case of fixed network junctions and rod centers. The relaxation time corresponding to this branch is  $\tau_r = (\zeta + 2\zeta_i)/(K_1 + 2K)$  at  $\vec{\theta} \rightarrow 0$ . Branch III is characterized at  $\vec{\theta} \rightarrow 0$  by in-phase *translational* mobility of the rods in adjacent cells when movements of network junctions and rod centers in the same cell are anti-phase (in contrast to the branch I). The characteristic time corresponding to such motion is  $\tau_{III} = \tau_t/(1 + 6\zeta/\zeta_N)$ . The relaxation times of all the branches are

strongly dependent on the viscoelastic parameters of the model, see Figures 5a–d.

Now, we note that the relaxation spectra plotted in Figures 5a–d have been calculated using the values of the elasticity constant,  $K$ , estimated by means of Equation (7) which includes the contribution of all the normal modes for the network. However, from Equation (9) it follows that there are normal modes (corresponding to the relaxation times  $\tau_r$  and  $\tau_i$ ) when the network junctions are immobile. The effects of these modes on the mobility of included rods have been analyzed separately by the authors in refs.<sup>[9,10]</sup> It was shown that the contribution of these modes leads to the following condition for the elasticity constant,  $K_{\text{fix}}$ , of the spring modeling the rod between fixed network junctions:

$$l^2 = h^2 \left( \frac{K_1}{K_1 + 2K_{\text{fix}}} \right)^2 + \frac{6kT}{K_1 + 2K_{\text{fix}}} \quad (13)$$

The value of  $K_{\text{fix}}$  can be different from the value of  $K$  calculated from Equation (7) which includes the contribution of all the normal modes, see Figures 6a–d. However, the choice of  $K$  or  $K_{\text{fix}}$  doesn't strongly influence the relaxation spectrum of the system. Indeed, according to Equation (9), all the relaxation times of the system depend on the constant  $K$  only through the parameter  $\tau_r = (\zeta + 2\zeta_1)/(K_1 + 2K)$ . But Figures 6a–d show that the choice of  $K$  or  $K_{\text{fix}}$  doesn't strongly change the value of the rotational relaxation time  $\tau_r$  since the ratio  $\tau_r^{(\text{fix})}/\tau_r$  is very close to unity. Here  $\tau_r^{(\text{fix})} = (\zeta + 2\zeta_1)/(K_1 + 2K_{\text{fix}})$ . Thus, we can use both above-mentioned approximations for estimating the quantity  $K$  since the choice of one of these approximations does not strongly change the relaxation times of the system.

The analysis of the different branches of the relaxation spectra shows that if we consider the motion of the rod (e.g. rotation

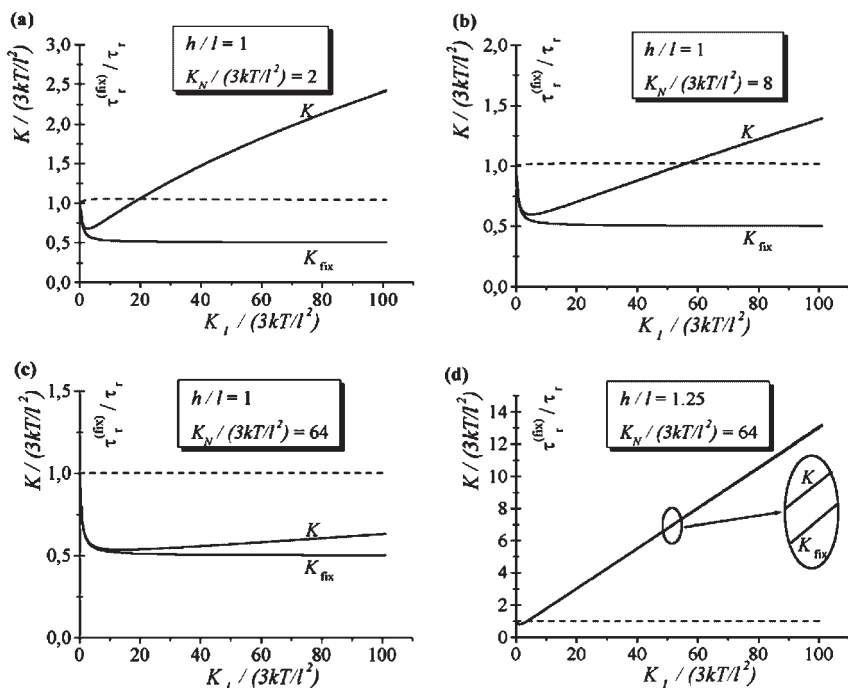


**Figure 6.**

The values of the elasticity constant of the spring modelling the rod in a polymer network with moving junctions ( $K$ , Equation (7)) and in a network with fixed junctions ( $K_{\text{fix}}$ , Equation (13)). Dashed lines show the ratio  $\tau_r^{(\text{fix})}/\tau_r$  where  $\tau_r = (\zeta + 2\zeta_1)/(K_1 + 2K)$  and  $\tau_r^{(\text{fix})} = (\zeta + 2\zeta_1)/(K_1 + 2K_{\text{fix}})$ .



mobility appearing in the correlation functions  $\langle \cos \vartheta(t) \cos \vartheta(0) \rangle$  or  $\langle \cos^2 \vartheta(t) \cos^2 \vartheta(0) \rangle$  monitored by the methods of dielectric<sup>[11]</sup> and NMR<sup>[13]</sup> relaxation, respectively, and also motions appearing in mechanical relaxation<sup>[12]</sup>) we can see overlapping or separation of different branches. Sometimes the maxima for different branches are also separated in the time or frequency scale.

Let us consider as an example the structure of the local motion appearing, e.g., in dielectric relaxation which is determined by the correlation function,  $\langle \cos \vartheta(t) \cos \vartheta(0) \rangle$ , see ref.<sup>[11]</sup> for details. Knowing the  $\theta$ -dependencies of the relaxation spectra we can calculate<sup>[11]</sup> the spectral density,  $L(\tau)$ , for the correlation function of  $\langle \cos \vartheta(t) \cos \vartheta(0) \rangle$ :

$$\frac{\langle \cos \vartheta(t) \cos \vartheta(0) \rangle - \langle \cos \vartheta(0) \rangle^2}{\langle \cos^2 \vartheta(0) \rangle - \langle \cos \vartheta(0) \rangle^2} = \int_0^\infty \exp[-t/\tau] \cdot L(\tau) d \ln \tau \quad (14)$$

The spectral density  $L(\tau)$  determines the frequency dependence of the dielectric loss factor  $\varepsilon''$  for polar rods with permanent dipole moments which are assumed to be directed parallel to the long axis of the rods:

$$\frac{\varepsilon''(\omega)}{\varepsilon_0 - \varepsilon_\infty} = \int_0^\infty \frac{\omega \tau}{1 + (\omega \tau)^2} \cdot L(\tau) d \ln \tau \quad (15)$$

The spectral density  $L(\tau)$  is presented in Figure 7 for relatively viscous network at high  $K_1$ . Each branch of the spectral density  $L(\tau)$  yields the contribution to the frequency dependence of  $\varepsilon''$ . At first, the orientational mobility of rods is determined by the branch of the relaxation spectrum with fixed junctions which is characterized by the time  $\tau_r$ . Some increments of the collective branches I, II and III also appear in this process. But if the network friction  $\zeta_N$  is very high the relaxation times of the collective branch I are also very high and can be separated from the relaxation times of other branches. In this case the dielectric loss factor can have two maxima – see

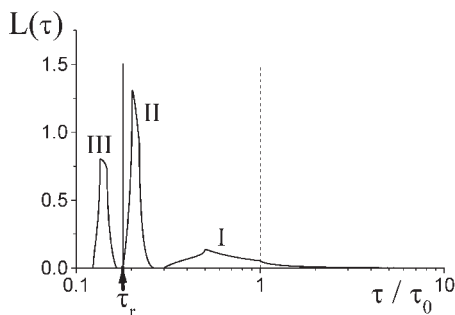


**Figure 7.**

The spectral density,  $L(\tau)$ , for a free rod (dashed line) and for a rod included into a polymer network (solid lines) at  $K_1/(3kT/P) = 5$ ,  $K_N/(3kT/P) = 4$ ,  $\zeta_N/\zeta = 10$ ,  $h/l = 2$ .  $\tau_0 = \zeta l^2/4kT$ .

Figure 8a. As parameter  $\zeta_N/\zeta$  increases, the relaxation times of the collective branch I increases and the low-frequency maximum of  $\varepsilon''(\omega)$  shifts toward low frequencies, see Figure 8a. The higher is  $\zeta_N/\zeta$  the lower are the amplitudes of both high- and low-frequency maxima of  $\varepsilon''(\omega)$ , Figure 8a.

The increment of the network motion depend also on the strength of the quasi-elastic interaction between the rods and network fragments,  $K_1$ . The increasing of  $K_1$  leads to the decrease of all relaxation times but the high-frequency maximum of  $\varepsilon''(\omega)$  determined by the relaxation with fixed junction shifts strongly to high frequency – see Figure 8b. If  $K_1$  (at given  $h \sim l$ ) is very high the amplitude of the short time motion at fixed junction is very small. In this case, the increment of low frequency network motions is very important. As a result (Figure 8b), with increasing parameter  $K_1$ , the height of the low-frequency maximum of  $\varepsilon''(\omega)$  increases, whereas the height of the high-frequency maximum, which corresponds to localized rod movements at fixed network junctions, decreases. The elasticity of the network chains,  $K_N$ , and chain stretching between junctions,  $h/l$ , also influence the frequency dependence of the dielectric loss factor,  $\varepsilon''(\omega)$ , see ref.<sup>[11]</sup> for details.

As it was found earlier by the authors,<sup>[13]</sup> the similar effects appear in the characteristics of NMR: in the spin-lattice relaxation



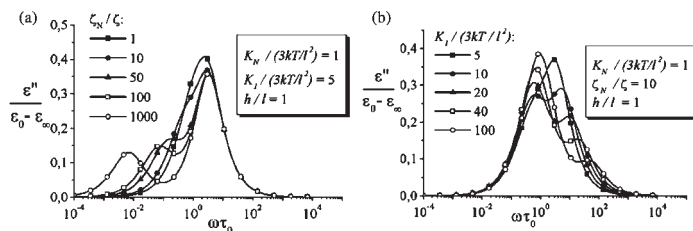


Figure 8.

The frequency dependences of the dielectric loss factor  $\varepsilon''(\omega)$  at varying values of the parameters  $\zeta_N/\zeta$  (a) and  $K_l/(3kT/l^2)$  (b).

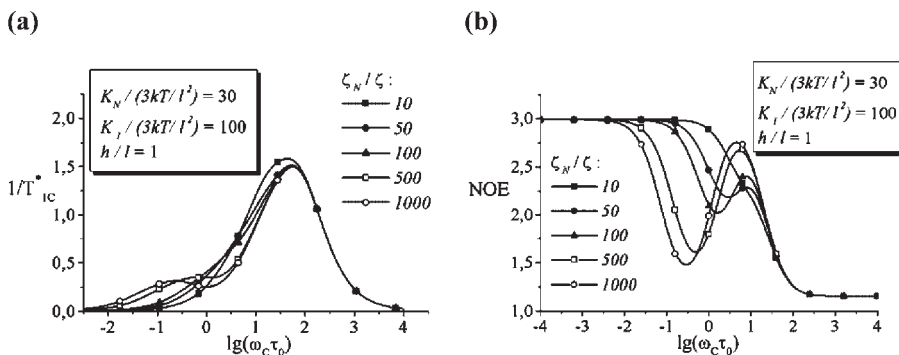


Figure 9.

The frequency dependences of  $1/T_{1C}^* = (10r_{CH}^6/\gamma_C^2\gamma_H^2\hbar^2) \cdot 1/T_{1C}$  and NOE for rods included into a polymer network at different values of the parameter  $\zeta_N/\zeta$ . Here  $r_{CH}$  is the distance between the nuclei of  $^{13}\text{C}$  and  $^1\text{H}$ ;  $\gamma_H$  and  $\gamma_C$  are the gyromagnetic ratios for nuclei  $^1\text{H}$  and  $^{13}\text{C}$ . The internuclear vector  $\vec{r}_{CH}$  is assumed to be directed along the rod-like particle.

time of the nuclei  $^{13}\text{C}$  ( $T_{1C}$ ) and in the nuclear Overhauser effect (NOE). As examples, Figures 9a and 9b illustrate the dependences of the  $T_{1C}$  and NOE on the resonance frequency of the nuclei  $^{13}\text{C}$  ( $\omega_C$ ) at varying values of  $\zeta_N/\zeta$ . One can see that at sufficiently high values of  $K_1$  and  $\zeta_N$  the frequency dependences of the  $T_{1C}$  and NOE can have two maxima due to separation of the collective long-scale branch from the localized rotational relaxation times of rods at fixed network junctions.

The dielectric and NMR relaxation are determined mainly by the rotational mobility of rods included into the network. As to translational vibrations of the rods in the network, they are at first controlled by the

branch with the relaxation time  $\tau_l$  at fixed junctions and by the collective branch III (Figures 5a–d). The amplitude of this motion depends strongly on  $K_1$ . At  $K_1 \rightarrow 0$  this amplitude tends to infinity and the translational motion of the rods is monitored strongly in mechanical relaxation (in dynamic modulus, see ref. [12]) in contrast to dielectric and NMR relaxation where the effects of this type of motion are very weak as it was mentioned above.

## Conclusion

The investigation of the structure of the “coarse-grained” visco-elastic model of a

polymer network with quasielastically included rod-like particles can give information about the relaxation spectra of this system depending on the interaction between rods and network, on the primary equilibrium and relaxation properties of the network and rods and on the degree of swelling of the network. The relaxation properties of the system can be applied to some relaxation phenomena, such as dielectric and NMR relaxation and other phenomena appearing in a polymer network with included hard rods.

**Acknowledgements:** This work was carried out with the financial support of the Russian Foundation of Basic Research (grant 05-03-32332), INTAS (projects 00-445, 04-83-2912) and Government of Saint-Petersburg.

[1] R. Rulken, G. Wegner, V. Enkelmann, M. Schutze, *Ber. Bunsenges. Phys. Chem.* **1996**, 100, 707.  
 [2] O. E. Philippova, R. Rulken, B. Y. Kovtunenkov, S. S. Abramchuk, A. R. Khokhlov, G. Wegner, *Macromolecules* **1998**, 31, 1168.  
 [3] R. Rulken, G. Wegner, T. Thurn-Albrecht, *Langmuir* **1999**, 15, 4022.  
 [4] M. Bockstaller, W. Koehler, G. Wegner, G. Fytas, *Macromolecules* **2001**, 34, 6353.  
 [5] Yu. D. Zaroslov, V. I. Gordely, A. I. Kuklin, A. H. Islamov, O. E. Philippova, A. R. Khokhlov, G. Wegner, *Macromolecules* **2002**, 35, 4466.

[6] Yu. Ya. Gotlib, A. A. Gurtovenko, I. A. Torchinskii, V. A. Shevelev, V. P. Toshchevnikov, *Macromolecular Symposia* **2003**, 191, 121.  
 [7] Yu. Ya. Gotlib, A. A. Gurtovenko, I. A. Torchinskii, V. A. Shevelev, V. P. Toshchevnikov, *Journal of Engineering Physics and Thermophysics*, **2003**, 76(3), 480.  
 [8] Yu. Ya. Gotlib, I. A. Torchinskii, V. P. Toshchevnikov, *Macromol. Theory Simul.* **2004**, 13(4), 303.  
 [9] Yu. Ya. Gotlib, A. A. Lezova, I. A. Torchinskii, V. P. Toshchevnikov, V. A. Shevelev, *Polymer Science, Ser. A*, **2005**, 47(7), 1203.  
 [10] Yu. Ya. Gotlib, A. A. Lezova, I. A. Torchinskii, *Polymer Science, Ser. A*, **2006**, 48(5), 498.  
 [11] V. P. Toshchevnikov, Yu. Ya. Gotlib, *Polymer Science, Ser. A*, **2006**, 48(6), 649.  
 [12] Yu. Ya. Gotlib, I. A. Torchinskii, V. P. Toshchevnikov, V. A. Shevelev, *Macromolecular Symposia*, **2006**, 237(1), 60.  
 [13] Yu. Ya. Gotlib, I. A. Torchinskii, V. P. Toshchevnikov, V. A. Shevelev, *Applied Magnetic Resonance* **2006**, 30(3–4), in press.  
 [14] Yu. Ya. Gotlib, A. A. Darinsky, L. I. Klushin, I. M. Neelov, *Acta Polymerica* **1984**, 35(3), 124.  
 [15] Yu. Ya. Gotlib, *Progress in Colloid and Polymer Science* **1989**, 80, 245.  
 [16] A. A. Darinskii, Yu. Ya. Gotlib, A. V. Lyulin, I. M. Neelov, *Polymer Science USSR. Ser. A*, **1992**, 34, 11.  
 [17] A. A. Darinskii, Yu. Ya. Gotlib, A. V. Lyulin, I. M. Neelov, *Polymer Science USSR. Ser. A*, **1994**, 36, 948.  
 [18] A. A. Gurtovenko, Yu. Ya. Gotlib, *Macromolecules* **1998**, 31(17), 5756.  
 [19] A. A. Gurtovenko, Yu. Ya. Gotlib, *Macromolecules* **2000**, 33(17), 6578.  
 [20] G. Ronca, *Polymer* **1979**, 20, 1321.